Up-link Multiple-user V-BLAST Optimal Detection Ordering with Service Differentiation

Tariq Al-Khasib, *Student Member, IEEE,* Lutz Lampe, *Senior Member, IEEE,*
and Hussein Alnuweiri, *Member, IEEE*

***Abstract*—In this paper, we introduce a new Differentiated Successive Interference Cancellation (DiffSIC) ordering technique for up-link multiple-user systems. Unlike classical SIC, DiffSIC is capable of differentiating users according to their priority or class of service by selecting a detection order that best fits the users' service profiles. In addition, DiffSIC is able to achieve the optimal SIC detection order that results in the best overall system performance. In order to develop DiffSIC, we introduce analytical methods towards finding instantaneous symbol error rates (SER) for the Zero Forcing SIC (ZF-SIC) and Minimum Mean Square Error SIC (MMSE-SIC) detectors. Furthermore, we devise two procedures to reduce the computational complexity associated with the computation of SER and the enumeration of detection orders. We present a number of numerical results which clearly demonstrate the ability of DiffSIC to accomplish service differentiation and overall performance improvement in general.**

***Index Terms*—Successive interference cancellation (SIC), V-BLAST, zero forcing (ZF) detector, user differentiation, symbol error rate (SER) analysis.**

I. Introduction

MULTIPLE-Input Multiple-Output (MIMO) techniques have been widely recognized as a means for improved performance of wireless communications. MIMO techniques provide additional spatial degrees of freedom that can result in several orders-of-magnitude increase in data rate and significant decrease in interference in point-to-point, point-to-multipoint and multipoint-to-point wireless transmission. In the latter case, different users can be viewed as different transmitting antennas, and Space-Time Multiple-User Detection (MUD) can be used at the base station to separate the signals from these users [1, 2]. Since optimal space-time MUD algorithms are often too complex and time consuming, linear and non-linear approximations of optimal algorithms are used. In particular, non-linear detectors using Successive Interference Cancellation (SIC) are powerful and significantly outperform linear detectors. In these detectors, the order of detection substantially affects the performance of individual users. The classical SIC detector is the Vertical Bell Laboratory Layered Space Time (V-BLAST) detector [3] that aims at finding the detection order that carries the least amount of error propagation.

In the context of a layered transmission approach, the Medium Access Control (MAC) layer is normally responsible for providing service differentiation through frame scheduling, while the Physical (PHY) layer's responsibility is to deliver the packets passed by the MAC layer with the least amount of errors. This concept has changed when researchers started to think across layers and noticed that getting the PHY layer involved in the packet scheduling effort could enhance the performance of the system dramatically [4]. The Channel State Dependent Packet Scheduling (CSDPS) [5] was one of the first schedulers to address this problem. But, this involvement always took place in the scheduling process of the MAC (i.e. the status from the PHY layer was used in the scheduling process of the MAC), and had nothing to do with PHY layer transmission and detection tools and algorithms that were used.

In this paper, we claim that the service differentiation process can take advantage of the PHY layer capabilities to gain more improvement at the user level. To this end, we propose a new SIC ordering algorithm that works at the base station of a multiple-user up-link system and can differentiate users in service by altering the detection sequence. In particular, this Differentiated SIC (DiffSIC) works in favor of high priority customers, while low priority users may experience a (short-term) performance degradation. DiffSIC considers Symbol Error Rate (SER) as the relevant performance measure, and therefore we also derive the necessary SER expressions in this paper. We note that an enhancement in SER, or interchangeably the Packet Error Rate (PER), performance of a user's communications link directly affects the performance of data communications over that link. In error-intolerant applications (commonly running over TCP/IP), such as file transfers, and web browsing, a more reliable link translates directly into less retransmissions which, in turn, means lower delay and higher efficiency. On the other hand, in applications such as voice or video over IP, certain levels of error can be tolerated as long as they do not extremely deteriorate the content quality to a point where it becomes noticeable by the end user. We present a number of simulation results which substantiate that DiffSIC is capable of changing link reliabilities according to the needs of such applications. We would like to emphasize that DiffSIC takes place at the base station and requires no involvement of

Manuscript received February 24, 2009; and revised September 27, 2009. This work was supported by the National Sciences and Engineering Research Council (NSERC) of Canada. The material in this paper was presented in part at the 2009 IEEE 70th Vehicular Technology Conference (VTC-Fall '09).

T. Al-Khasib and L. Lampe are with the Department of Electrical and Computer Engineering, University of British Columbia, Vancouver, BC, Canada. H. Alnuweiri is with the Department of Electrical and Computer Engineering, Texas A&M University, Qatar. (e-mail: tariqa@ece.ubc.ca, lampe@ece.ubc.ca, hussein.alnuweiri@qatar.tamu.edu).

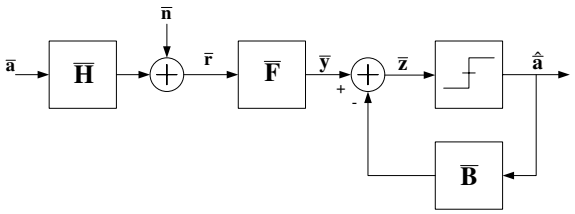

Fig. 1: Block diagram of the equivalent real-valued transmission system using a SIC detector.

or feedback to the users. If such a feedback is available or used for user differentiation anyway [6, 7], DiffSIC could still be applied as an additional fine-grain service differentiation tool. Also, through a feedback channel, high priority users can be advised to use a higher signal constellation size to take full advantage of the improved signal quality they enjoy at the receiver.

Organization: The rest of this paper is organized as follows. Section II presents the system model under consideration, along with the SIC detector structure at the receiver. In Section III we introduce the new detection ordering algorithm, DiffSIC, and the required analysis of the instantaneous SER performance of Zero Forcing SIC (ZF-SIC) and Minimum Mean Square Error SIC (MMSE-SIC) receivers. In Section IV, we introduce two techniques towards reducing the computational complexity associated with the algorithm. We then investigate the effect of channel estimation errors on DiffSIC performance in Section V. In Section VI we present and discuss selected performance results obtained through analysis and Monte Carlo simulations and we conclude the paper in Section VII.

Notation: In this paper, we use bold upper case and lower case letters for matrices and vectors, respectively. $[\cdot]^T$, $[\cdot]^H$, and $[\cdot]^{-1}$ denote transposition, Hermitian transposition, and matrix inversion, respectively. The notation $\|\cdot\|_2$ refers to the ℓ^2-norm of a vector while $\boldsymbol{I}_n$ denotes the $n\times n$ identity matrix. Finally, $\Re(\cdot)$ and $\Im(\cdot)$ refer to the real and imaginary parts of a complex number, respectively.

II. System Model

We consider the up-link of a multiple-user system, where each user is equipped with a single transmit antenna, while the base station has M_r receive antennas. Each user acts as a single antenna of a MIMO transmitter, and space is utilized by allowing M_t users to communicate simultaneously to the base station such that $M_\mathrm{t} \leq M_\mathrm{r}$[1]. The up-link transmitters use square M-ary Quadrature Amplitude Modulation (QAM) constellations and SIC is used at the base station to separate different users. The block diagram of the equivalent discrete-time transmission system is shown in Figure 1.

The received signal at the base station can be represented in the complex baseband vector form as

$$\boldsymbol{r} = \boldsymbol{H}\boldsymbol{a} + \boldsymbol{n}, \tag{1}$$

[1]The ideas presented in this paper are readily extended to multiple-user MIMO systems where individual users have multiple antennas and different applications/streams that might have different service requirements.

where $\boldsymbol{r} = [r_1 \cdots r_{M_\mathrm{r}}]^T$ is the received signal vector, $\boldsymbol{H}$ is the $M_\mathrm{r} \times M_\mathrm{t}$ channel matrix, $\boldsymbol{a} = [a_1 \cdots a_{M_\mathrm{t}}]^T$ is the transmitted QAM signal vector with average element-wise symbol energy E_s, and $\boldsymbol{n} = [n_1 \cdots n_{M_\mathrm{r}}]^T$ is the i.i.d. circularly symmetric complex Gaussian noise vector with covariance matrix $\sigma_n^2 \boldsymbol{I}_{M_\mathrm{r}}$. The transmission model in (1) can also be written in its equivalent real-valued format

$$\bar{\boldsymbol{r}} = \bar{\boldsymbol{H}}\bar{\boldsymbol{a}} + \bar{\boldsymbol{n}} \tag{2}$$

where

$$\bar{\boldsymbol{r}} = \begin{bmatrix} \Re(r_1) \\ \Im(r_1) \\ \vdots \\ \Re(r_{M_\mathrm{r}}) \\ \Im(r_{M_\mathrm{r}}) \end{bmatrix}, \; \bar{\boldsymbol{a}} = \begin{bmatrix} \Re(a_1) \\ \Im(a_1) \\ \vdots \\ \Re(a_{M_\mathrm{t}}) \\ \Im(a_{M_\mathrm{t}}) \end{bmatrix}, \; \bar{\boldsymbol{n}} = \begin{bmatrix} \Re(n_1) \\ \Im(n_1) \\ \vdots \\ \Re(n_{M_\mathrm{r}}) \\ \Im(n_{M_\mathrm{r}}) \end{bmatrix},$$

and

$$\bar{\boldsymbol{H}} = \begin{bmatrix} \Re(h_{1,1}) & -\Im(h_{1,1}) & \cdots & \Re(h_{1,M_\mathrm{t}}) & -\Im(h_{1,M_\mathrm{t}}) \\ \Im(h_{1,1}) & \Re(h_{1,1}) & \cdots & \Im(h_{1,M_\mathrm{t}}) & \Re(h_{1,M_\mathrm{t}}) \\ \vdots & \vdots & \ddots & \vdots & \vdots \\ \Re(h_{M_\mathrm{r},1}) & -\Im(h_{M_\mathrm{r},1}) & \cdots & \Re(h_{M_\mathrm{r},M_\mathrm{t}}) & -\Im(h_{M_\mathrm{r},M_\mathrm{t}}) \\ \Im(h_{M_\mathrm{r},1}) & \Re(h_{M_\mathrm{r},1}) & \cdots & \Im(h_{M_\mathrm{r},M_\mathrm{t}}) & \Re(h_{M_\mathrm{r},M_\mathrm{t}}) \end{bmatrix}.$$

Thus the $M_\mathrm{t}\times M_\mathrm{r}$ M-ary QAM system gets transformed into a $2M_\mathrm{t} \times 2M_\mathrm{r}$ real valued L-ary Pulse Amplitude Modulation (PAM) system where $L = \sqrt{M}$. The signal-to-noise power ratio (SNR) of the equivalent system remains intact since both the noise and symbol energies get divided by 2.

The signal $\bar{\boldsymbol{r}}$ is processed at the receiver by a SIC detector to separate signals from different users. The detector is illustrated in Figure 1 and can be expressed as [8, Ch. 10.3.4]

$$\bar{\boldsymbol{z}} = \bar{\boldsymbol{F}}\bar{\boldsymbol{r}} - \bar{\boldsymbol{B}}\hat{\bar{\boldsymbol{a}}}, \tag{3}$$

where $\bar{\boldsymbol{F}}, \bar{\boldsymbol{B}}$ and $\hat{\bar{\boldsymbol{a}}}$ are the $2M_\mathrm{t} \times 2M_\mathrm{r}$ matrix forward filter, the $2M_\mathrm{t} \times 2M_\mathrm{t}$ strictly lower triangular matrix feedback filter, and the vector of $2M_\mathrm{t}$ detected symbols, respectively.

In SIC detectors, the order of detection greatly affects the performance of individual users. The user that is detected first receives no gain from the SIC, while the user detected last achieves its best performance *if* correct decisions were assumed. Given a channel realization, there is always a detection order that gives the best average performance. In V-BLAST, instantaneous post-detection SNRs are used to achieve a detection order in a sequential manner [3]. As we will see later in this paper, this criterion does not always result in the best order, in terms of SER performance, although it gives a very good approximation considering its low processing requirements.

It was shown in [9, 10] that when considering the real-valued model in (2) shaping the equivalent real-valued channel matrix such that the real and imaginary parts of one transmitter get detected in sequence renders these two parts of the signal independent. This in turn reduces the complexity of computing the matrix filters $\bar{\boldsymbol{F}}$ and $\bar{\boldsymbol{B}}$ and limits the number of possible orders of detection back to $M_\mathrm{t}!$. The equivalent model in (2) will be used throughout this paper with the assumption that the real and imaginary parts of one user are detected in sequence.

III. DIFFSIC ORDERING ALGORITHM

As it was mentioned earlier, in SIC receivers, applying the detection order that leads to the best *average* system performance might not always be desirable. Users with high priority can be given an advantage by choosing detection orders that work in their favor. The proposed Differentiated Successive Interference Cancellation (DiffSIC) algorithm gives the flexibility of differentiating users according to their class of service. DiffSIC exploits the predicted SER performance to determine the order of detection. Therefore, we first derive SER expressions for SIC taking error propagation into account. Then, we present the DiffSIC algorithm and its adaptation to the case when multiple detection chains are employed at the receiver. As in the related literature, e.g., [11–13], we mainly focus on ZF-SIC for its better analytical tractability, but the extension to MMSE-SIC is also shown.

A. SER Analysis for ZF-SIC Detectors

The following analysis is similar to those in [11, 13], but adapted to the real-valued transmission model in (2) and with an efficient extension to non-binary transmission, which renders the computational complexity of the final expression independent of the constellation size M.

Given a channel realization $\boldsymbol{H}$, the error probability for M-ary QAM transmission at the i-th layer, $1 \leq i \leq M_{\mathrm{t}}$, can be calculated as

$$P_{i|\boldsymbol{H}}^{M-QAM} = 1 - \left(1 - P_{2i-1|\bar{\boldsymbol{H}}}^{L-PAM}\right)\left(1 - P_{2i|\bar{\boldsymbol{H}}}^{L-PAM}\right), \quad (4)$$

where $P_{2i-1|\bar{\boldsymbol{H}}}^{L-PAM}$ and $P_{2i|\bar{\boldsymbol{H}}}^{L-PAM}$ are the error probabilities of the equivalent real and imaginary L-ary PAM signals, respectively. Note that the i-th layer of the complex-valued system model in (1) corresponds to the $(2i-1)$-st and $2i$-th layers of the equivalent real-valued system model in (2). The error probability for the real-valued model can be written as

$$P_{i|\bar{\boldsymbol{H}}}^{L-PAM} = \sum_{\boldsymbol{e}_{i-1} \in \boldsymbol{\mathcal{E}}_{i-1}} P_{i|\boldsymbol{e}_{i-1}} \Pr(\boldsymbol{e}_{i-1}), \quad (5)$$

where $\boldsymbol{\mathcal{E}}_{i-1}$ is the set of all possible error sequences $\boldsymbol{e}_{i-1} = [e_1, e_2, ..., e_{i-1}]$ of layers prior to layer i, $P_{i|\boldsymbol{e}_{i-1}}$ is the probability of error at the i-th step given the error sequence $\boldsymbol{e}_{i-1}$, and $\Pr(\boldsymbol{e}_{i-1})$ is the probability that such an error sequence occurs.

To find the conditional error probability $P_{i|\boldsymbol{e}_{i-1}}$, we need to consider the detector output $\bar{\boldsymbol{z}}$ given in (3). Since $\bar{\boldsymbol{B}}$ is strictly lower triangular, the decision variable $\bar{z}_i$ at the i-th layer can be written as

$$\bar{z}_i = \bar{a}_i + \bar{\boldsymbol{f}}_i \bar{\boldsymbol{n}} + \sum_{k=1}^{i-1} \bar{b}_{ik}\left(\bar{a}_k - \hat{\bar{a}}_k\right) = \bar{a}_i + \bar{\boldsymbol{f}}_i \bar{\boldsymbol{n}} + \sum_{k=1}^{i-1} \bar{b}_{ik} e_k, \quad (6)$$

where $\bar{\boldsymbol{f}}_i$ is the i-th row of the matrix forward filter $\bar{\boldsymbol{F}}$ and $\bar{b}_{ik}$ is the element at the i-th row and k-th column of the matrix feedback filter $\bar{\boldsymbol{B}}$[2]. Since the rows of $\bar{\boldsymbol{F}}$ are orthogonal in case of ZF-SIC, the decision variables $\bar{z}_i$ at different layers are independent for a given $\boldsymbol{e}_{i-1}$.

For non-binary signal constellations, we make the assumption that errors between nearest-neighbor signal points with minimum Euclidean distance $d_{\min} = \sqrt{\frac{6}{M-1}E_s}$ dominate the performance. This limits the set of error symbols e_i to $\mathcal{E}_i = \{-d_{\min}, 0, +d_{\min}\}$ and renders the complexity for computing the SER, and thus the DiffSIC algorithm introduced below, independent of the size M of the signal constellation used by the users[3]. Simulation results in Section VI show that such an assumption is reasonable for SNR values where communication systems usually operate. Then, from (6), we derive in the Appendix that $P_{i|\boldsymbol{e}_{i-1}}$ can be written as

$$P_{i|\boldsymbol{e}_{i-1}} = P_{i|\boldsymbol{e}_{i-1}}^{(1)} + P_{i|\boldsymbol{e}_{i-1}}^{(2)}, \quad (7)$$

where

$$P_{i|\boldsymbol{e}_{i-1}}^{(1)} = \left(\frac{L-1}{L}\right) Q\left(\frac{d_{\min}/2 + \sum_{k=1}^{i-1} \bar{b}_{ik} e_k}{\sqrt{\sum_{j=1}^{M_{\mathrm{r}}} \bar{f}_{ij}^2 \sigma_n^2/2}}\right), \quad (8)$$

and

$$P_{i|\boldsymbol{e}_{i-1}}^{(2)} = \left(\frac{L-1}{L}\right) Q\left(\frac{d_{\min}/2 - \sum_{k=1}^{i-1} \bar{b}_{ik} e_k}{\sqrt{\sum_{j=1}^{M_{\mathrm{r}}} \bar{f}_{ij}^2 \sigma_n^2/2}}\right). \quad (9)$$

In (8) and (9), $\bar{f}_{ij}$ refers to the element at the i-th row and j-th column of the forward filter $\bar{\boldsymbol{F}}$ and $Q(\cdot)$ is the complementary cumulative distribution function of a Gaussian random variable. Finally, we note that $\Pr(\boldsymbol{e}_{i-1})$ follows from the recursion

$$\Pr(\boldsymbol{e}_{i-1}) = \prod_{k=1}^{i-1} \Pr(e_k | \boldsymbol{e}_{k-1}), \quad (10)$$

where

$$\Pr(e_k|\boldsymbol{e}_{k-1}) = \begin{cases} 1 - P_{k|\boldsymbol{e}_{k-1}} & , \ e_k = 0, \\ P_{k|\boldsymbol{e}_{k-1}}^{(1)} & , \ e_k = +d_{\min}, \\ P_{k|\boldsymbol{e}_{k-1}}^{(2)} & , \ e_k = -d_{\min}. \end{cases} \quad (11)$$

[2]The forward filter $\bar{\boldsymbol{F}}$ can be derived using the Cholesky decomposition of the Hermitian matrix $\bar{\boldsymbol{R}} = \bar{\boldsymbol{H}}^H \bar{\boldsymbol{H}} = \bar{\boldsymbol{G}}^H \bar{\boldsymbol{G}}$, where $\bar{\boldsymbol{G}}$ is a lower triangular matrix with real and positive diagonal elements. $\bar{\boldsymbol{G}}$ can be further decomposed according to $\bar{\boldsymbol{G}} = \bar{\boldsymbol{\Gamma}}\bar{\boldsymbol{M}}$, where $\bar{\boldsymbol{\Gamma}}$ is diagonal with real and positive elements, and $\bar{\boldsymbol{M}}$ is lower triangular and monic. The forward filter $\bar{\boldsymbol{F}}$ can then be written as $\bar{\boldsymbol{F}} = \bar{\boldsymbol{\Gamma}}^{-1}\bar{\boldsymbol{G}}^{-H}\bar{\boldsymbol{H}}^H$, and the feedback matrix $\bar{\boldsymbol{B}}$ is the strictly lower triangular matrix such that $\bar{\boldsymbol{B}} = \bar{\boldsymbol{M}} - \boldsymbol{I}_{2M_{\mathrm{t}}}$. See [8, Ch. 10.3.4] for full details

[3]Here we assume that all users use that same constellation size. Nevertheless, the analysis is still applicable if different constellation sizes were used by different users as long as $d_{\min}$ is adjusted accordingly

B. DiffSIC Ordering Algorithm

The DiffSIC algorithm utilizes the SER expression (4) to determine the order of detection that best fits the service profile of different users. We first define the set of permutation matrices $\{\boldsymbol{P}_\ell | \ell = 1, \ldots, M_\mathrm{t}!\}$ corresponding to all possible channel detection orders such that $\boldsymbol{H}_\ell = \boldsymbol{H}\boldsymbol{P}_\ell$ is the ordered channel matrix. Then, for each detection order ℓ we compute the cost X_ℓ associated with this detection order as

$$X_\ell = \sum_{i=1}^{M_\mathrm{t}} c_i \; P_{i|\boldsymbol{H}_\ell}^{M-QAM}. \tag{12}$$

The contribution from user i to the cost X_ℓ is given by means of its SER $P_{i|\boldsymbol{H}_\ell}^{M-QAM}$ and the priority indicator c_i. The optimal order ℓ_{opt} can then be found as

$$\ell_{opt} = \underset{\ell}{\operatorname{argmin}}\, X_\ell. \tag{13}$$

The choice of the priority indicator vector $\boldsymbol{c} = [c_1, c_2, ..., c_{M_\mathrm{t}}]$ is done at higher layers and is based on the service profiles of users. Without loss of generality we limit c_i such that $c_i \in [0, 1]$ with 1 being the highest priority. The different priority classes essentially determine how greedy the algorithm should be to achieve the performance differentiation. The larger the difference between high priority and low priority assignments, the greedier the algorithm, and the better the performance of high priority users. Clearly, at the same time, DiffSIC may deteriorate the performance of low priority and best effort users $(c_i = 0)$.

The computational complexity of the DiffSIC algorithm lies in the repeated evaluation of the SER expression in (4). While the expression itself can be written in terms of elementary functions (e.g., using exponential approximations for the error function [14]), the number of possible error events $(3^{2(M_\mathrm{t}-1)})$ and orderings $(M_\mathrm{t}!)$ render the detection complexity larger than for regular V-BLAST especially for large dimensions M_t. We argue that this extra complexity may be affordable, especially in slowly time-varying channels, since DiffSIC is executed only infrequently compared to the detection process. This is decidedly different from ordering based on individual received vectors as advocated in e.g. [15]. Furthermore, the complexity of DiffSIC can significantly be reduced by approximating the calculation of $P_{i|\boldsymbol{H}_\ell}^{M-QAM}$ in (4) focusing on dominant error events or by using a subset of the total number of detection orders available. Such approximations are discussed in detail in Section IV.

C. Multiple Detection Chains

In the case where the receiver has the capacity to employ multiple SIC chains, a different order of detection can be exploited per chain and DiffSIC can be used to simultaneously work in favor of multiple users. The parallel use of several SIC detectors with different orders is known from multiuser detection for code-division multiple access (CDMA) under the name of parallel arbitrated search for interference cancellation (PASIC) [16, 17]. Different from PASIC, here we do not apply parallel detectors to arbitrate among candidate symbol estimates obtained with different pre-selected orders. Instead, DiffSIC chooses different orders of detection to achieve the best available performance for each user given a channel matrix $\boldsymbol{H}$. Results shown in Section VI demonstrate the performance benefits that are obtained with multiple detection chains.

D. Extension to MMSE-SIC

The DiffSIC algorithm is also readily extendable to Minimum Mean Square Error SIC (MMSE-SIC) receivers. Such an extension primarily depends on the availability of instantaneous SER estimates for MMSE-SIC receivers.

The decision variable for MMSE-SIC detection at layer i can be written as

$$\bar{z}_i = \sum_{k=i}^{2M_\mathrm{t}} \bar{m}_{ik}\bar{a}_k + \sum_{k=1}^{i-1} \bar{b}_{ik}e_k + \tilde{\bar{n}}_i, \tag{14}$$

where $\bar{m}_{ik}$ is the element in the i-th row and k-th column of $\bar{\boldsymbol{M}}$ and $\tilde{\bar{n}}_i = \bar{\boldsymbol{f}}_i\bar{\boldsymbol{n}}$ [4]. Different from ZF-SIC (cf. Eq. (6)), the MMSE forward filter $\boldsymbol{F}$ (i) does not transform the channel $\boldsymbol{H}$ into a monic and causal transfer function and (ii) the elements of the noise vector $\tilde{\bar{\boldsymbol{n}}} = [\tilde{\bar{n}}_1, \ldots, \tilde{\bar{n}}_{2M_\mathrm{t}}] = \bar{\boldsymbol{F}}\bar{\boldsymbol{n}}$ are correlated. Hence, the instantaneous SER analysis for MMSE-SIC detectors is different from that for ZF-SIC detectors in two aspects. First, the noise correlation increases the dependency between layers beyond the error propagation problem. Second, the imperfect interference suppression renders the error rate at a layer dependent on higher, yet to be detected, layers.

Taking the two mentioned effects into account, the error probability for MMSE-SIC at the i-th layer in (5) is given by

$$P_{i|\bar{\boldsymbol{H}}}^{L-PAM} = \sum_{\boldsymbol{a}_{i+1}\in\boldsymbol{\mathcal{A}}_{i+1}} \sum_{\boldsymbol{e}_{i-1}\in\boldsymbol{\mathcal{E}}_{i-1}} P_{i|\boldsymbol{e}_{i-1},\boldsymbol{a}_{i+1}} \Pr(\boldsymbol{e}_{i-1}) \Pr(\boldsymbol{a}_{i+1}), \tag{15}$$

where $\boldsymbol{\mathcal{A}}_{i+1}$ is the set of all possible L-PAM symbol sequences $\boldsymbol{a}_{i+1} = [a_{i+1}, ..., a_{2M_\mathrm{t}}]$ of layers to be detected and $P_{i|\boldsymbol{e}_{i-1},\boldsymbol{a}_{i+1}}$ is the probability of error at layer i given the error and symbol sequences $\boldsymbol{e}_{i-1}$ and $\boldsymbol{a}_{i+1}$. $P_{i|\bar{\boldsymbol{H}}}^{L-PAM}$ in (15) can be rewritten as

$$P_{i|\bar{\boldsymbol{H}}}^{L-PAM} = \frac{1}{L^{2M_\mathrm{t}-i}} \sum_{\boldsymbol{a}_{i+1}\in\boldsymbol{\mathcal{A}}_{i+1}} \sum_{\boldsymbol{e}_{i-1}\in\boldsymbol{\mathcal{E}}_{i-1}} P_{i,\boldsymbol{e}_{i-1}|\boldsymbol{a}_{i+1}}, \tag{16}$$

where $P_{i,\boldsymbol{e}_{i-1}|\boldsymbol{a}_{i+1}}$ is the joint error probability given the symbol sequence $\boldsymbol{a}_{i+1}$. $P_{i,\boldsymbol{e}_{i-1}|\boldsymbol{a}_{i+1}}$ can be calculated as

$$P_{i,\boldsymbol{e}_{i-1}|\boldsymbol{a}_{i+1}} = \left(\frac{1}{2}\prod_{k=1}^{i-1}(\alpha_k)\right) \left\{ \int_{\boldsymbol{\mathcal{D}}_{\boldsymbol{e}_{i-1},\boldsymbol{a}_{i+1}}^{(1)}} p(\tilde{\bar{\boldsymbol{n}}}_i)\, d\tilde{\bar{\boldsymbol{n}}}_i + \int_{\boldsymbol{\mathcal{D}}_{\boldsymbol{e}_{i-1},\boldsymbol{a}_{i+1}}^{(2)}} p(\tilde{\bar{\boldsymbol{n}}}_i)\, d\tilde{\bar{\boldsymbol{n}}}_i \right\}, \tag{17}$$

where $\tilde{\bar{\boldsymbol{n}}}_i = [\tilde{\bar{n}}_1, \ldots, \tilde{\bar{n}}_i]$, α_k is equal to 1 when $e_k = 0$ and $(L-1)/L$ otherwise, $p(\tilde{\bar{\boldsymbol{n}}}_i)$ is the probability density function

[4] For MMSE-SIC, the matrices $\bar{\boldsymbol{F}}$, $\bar{\boldsymbol{B}}$ and $\bar{\boldsymbol{M}}$ can be derived using a similar technique to the one described in III-A. The only difference is that $\bar{\boldsymbol{R}}$ has to be replaced by the matrix $\bar{\boldsymbol{R}} = \bar{\boldsymbol{H}}^H\bar{\boldsymbol{H}} + \sigma_n^2\boldsymbol{I}_{M_\mathrm{t}}$

(pdf) of $\tilde{\tilde{\boldsymbol{n}}}_i$, and $\boldsymbol{\mathcal{D}}^{(1,2)}_{\boldsymbol{e}_{i-1},\boldsymbol{a}_{i+1}}$ are the noise regions that lead to an error at layer i given $\boldsymbol{e}_{i-1}$ and $\boldsymbol{a}_{i+1}$ in both directions of the constellation point. The i-variate noise pdf is given by

$$p(\tilde{\tilde{\boldsymbol{n}}}_i) = \frac{1}{(2\pi)^{i/2}\sqrt{|\boldsymbol{M}_i|}} \exp\left(-\frac{1}{2}\tilde{\tilde{\boldsymbol{n}}}_i^T \boldsymbol{M}_i^{-1} \tilde{\tilde{\boldsymbol{n}}}_i\right), \qquad (18)$$

where $\boldsymbol{M}_i = \sigma_{\tilde{n}}^2 \bar{\boldsymbol{F}}_i \bar{\boldsymbol{F}}_i^T$ is the $i \times i$ noise covariance matrix and $\bar{\boldsymbol{F}}_i$ contains the first i rows of $\bar{\boldsymbol{F}}$. Evaluation of (17) in closed form is not possible. However, using again the nearest-neighbor-error approximation, the regions $\boldsymbol{\mathcal{D}}^{(1,2)}_{\boldsymbol{e}_{i-1},\boldsymbol{a}_{i+1}}$ are composed of a positive and negative orthant, and for this case several approximations for (17) have been proposed in literature, e.g. [18–20]. Here we adopt the method by Joe [20] that utilizes conditional expectations and regression with binary variables to approximate multivariate normal probabilities for rectangular regions. This approximation is sufficiently accurate and fast to compute (please refer to [20] for details). Thus, by substituting (15) into (4) we obtain a semi-analytical expression to quickly evaluate the SER for MMSE-SIC systems with a moderate number of users.

Further simplifications tackling complexity due to the averaging over $\boldsymbol{a}_{i+1}$ in (15) are possible but not pursued here. Instead, in the following section we introduce some approximations to lower the complexity of DiffSIC with respect to the number of error vectors and detection orders that need to be considered.

IV. Reduced Complexity Approximations for DiffSIC

The computational complexity of the optimal DiffSIC algorithm introduced in Section III has two main contributors, namely the cost of calculating the SER in (4) and the number of detection orders explored by the algorithm. Therefore, in this section, we present two simplifications that will help to reduce the cost of SER computation and the number of enumerated detection orders. These can be applied separately or in combination to lower the computational complexity. Furthermore, while the simplifications are applicable to both ZF- and MMSE-SIC, for clarity of exposition we restrict our attention to ZF-SIC receivers.

A. Low-Complexity SER Approximation

The complexity of calculating the SER in (5) grows exponentially with the number of layers, since the number of error sequences in the set $\boldsymbol{\mathcal{E}}_{i-1} = \{-d_{\min}, 0, +d_{\min}\}^{i-1}$ is equal to 3^{i-1}. In this section we introduce a reduced complexity approximation of this calculation by employing an effective subset $\boldsymbol{\Psi}_{i-1} \subset \boldsymbol{\mathcal{E}}_{i-1}$. In [13, 21] it was suggested that, on average, errors at the first layer have a dominant effect on the performance of subsequent layers. Thus, the dominant contributions to the error probability at layer i are coming from error sequences in $\boldsymbol{e}_{i-1} \in \boldsymbol{\Psi}_{i-1} = \{-d_{\min}, 0, +d_{\min}\} \times \{0\}^{i-2}$ that have errors only at the first step.

While the conclusions in [13, 21] are intuitively valid, they are not necessarily true for every channel realization nor will they lead to the best approach towards reduction in SER computational complexity as will exemplarily be shown in Section VI. We generalize the suggestion in [13, 21] in that we select the subset $\boldsymbol{\Psi}_{i-1}$ of error sequences that dominate the sum in (5). We limit the size $|\boldsymbol{\Psi}_{i-1}|$ to a predefined threshold N_{i-1} and thus control and reduce the algorithm's complexity by limiting the number of evaluations of (7). This approximate SER calculation is formalized in Table I.

TABLE I: Approximate SER calculation

Input: i, $\boldsymbol{H}_\ell$, N_{i-1}
Output: $P^{L-PAM}_{i|\bar{\boldsymbol{H}}}$

1: // Initialize set of error sequences
2: $\boldsymbol{\Psi}_{i-1} = \left\{\boldsymbol{e}^1_{i-1}\right\} = \{\boldsymbol{0}_{i-1}\}$
3: // Initialize error sequence count
4: $J = 1$
5: Calculate $P_{k|\boldsymbol{e}^1_{k-1}}$ for each $k \in \{1, 2, \cdots, i\}$
6: // Initialize SER estimate and decision matrix $\boldsymbol{E}$
7: $P^{L-PAM}_{i|\bar{\boldsymbol{H}}} = P_{i|\boldsymbol{e}^1_{i-1}} \Pr(\boldsymbol{e}^1_{i-1})$,
8: $\boldsymbol{E}(k,1) = P_{k|\boldsymbol{e}^1_{k-1}} \Pr(\boldsymbol{e}^1_{k-1})$ for each $k \in \{1, 2, \cdots, i-1\}$
9: **while** $(J < N_{i-1})$ **do**
10: // Find dominant error event, i.e., the error event that is most likely to happen
11: $[\hat{k}, \hat{j}] = \underset{k \in \{1,\ldots,i-1\}, j \in \{1,\ldots,J\}}{\operatorname{argmax}} \{\boldsymbol{E}(k,j)\}$
12: $\boldsymbol{E}(\hat{k}, \hat{j}) = -1$
13: // Branch error sequence at layer $\hat{k}$, which gives two new sequences
14: $\boldsymbol{e}^{J+1} = [\boldsymbol{e}^{\hat{j}}_{k-1}, -d_{\min}, \boldsymbol{0}_{i-k}]$, $\boldsymbol{e}^{J+2} = [\boldsymbol{e}^{\hat{j}}_{k-1}, +d_{\min}, \boldsymbol{0}_{i-k}]$, $\boldsymbol{\Psi}_{i-1} := \left\{\boldsymbol{\Psi}_{i-1}, \boldsymbol{e}^{J+1}, \boldsymbol{e}^{J+2}\right\}$
15: Calculate $P_{k|\boldsymbol{e}^j_{k-1}}$ for each $k \in \{\hat{k}+1, \cdots, i\}$ and $j \in \{J+1, J+2\}$
16: $\boldsymbol{E}(k,j) = -1$ for each $k \in \{1, \cdots, \hat{k}\}$ and $j \in \{J+1, J+2\}$
17: $\boldsymbol{E}(k,j) = P_{k|\boldsymbol{e}^j_{k-1}} \Pr(\boldsymbol{e}^j_{k-1})$ for each $k \in \{\hat{k}+1, \cdots, i-1\}$ and $j \in \{J+1, J+2\}$
18: // Update the SER estimate and error sequence count
19: $P^{L-PAM}_{i|\bar{\boldsymbol{H}}} := P^{L-PAM}_{i|\bar{\boldsymbol{H}}} + P_{i|\boldsymbol{e}^{J+1}_{i-1}} \Pr(\boldsymbol{e}^{J+1}_{i-1}) + P_{i|\boldsymbol{e}^{J+2}_{i-1}} \Pr(\boldsymbol{e}^{J+2}_{i-1})$
20: // Update error sequence count
21: $J := J + 2$
22: **end while**

In this approximation we use the fact that the higher the probability of error at one layer, the larger its influence in determining the dominant terms in the error calculation of subsequent layers. Thus, after scanning the initial calculation of errors at every layer assuming no previous errors (Table I, line 8), the algorithm branches the error sequence that is most likely to occur. That is, the most likely error event with sequence $[\boldsymbol{e}_{k-1}, \boldsymbol{0}_{i-k+1}]$ is followed-up by also considering the sequences $[\boldsymbol{e}_{k-1}, -d_{\min}, \boldsymbol{0}_{i-k}]$ and $[\boldsymbol{e}_{k-1}, +d_{\min}, \boldsymbol{0}_{i-k}]$ for error rate calculation (Table I, lines 14-17). This is extremely helpful, especially when the exact probabilities of error are not needed. We use this algorithm to approximate the cost function in (12). Results in Section VI confirm that the approximation in Table I can significantly reduce the amount of calculations needed and preserve the gains of DiffSIC at the same time. The amount of savings in computational complexity depends mainly on the number N_{i-1} and can be quantified as $\frac{N_{i-1}}{3^{i-1}} \times 100\%$.

B. Approximation for Selecting Order of Detection

The number of available detection orders grows factorially with the number of layers. Thus, at a certain level, it becomes impractical for DiffSIC to consider all possible detection orders when looking for the optimal order that best serves the differentiated needs of users. In this section we describe a reduced complexity search algorithm that can be adjusted to the computational capabilities of the receiver's processor. The algorithm narrows the set of detection orders to be considered down to a predetermined maximum number of orders $N_{\max}$, where DiffSIC can kick back in and choose the best order among the shortened list.

The proposed heuristic solution to reduce the number of orders to be considered by the DiffSIC algorithm is to fix the first F users in the detection chain such that $(M_{\mathrm{t}} - F)! \leq N_{\max}$. This is accomplished by choosing these first users of the detection sequence similar to the way V-BLAST orders users with the exception that a scaled version of the instantaneous post-detection SNRs is applied, where the scaling factor decreases with user priority. Thus, high priority users are pushed towards the end of the detection chain. The rationale for this is that even though error propagation in SIC eliminates any diversity gains for higher layers, SNR gains when moving from lower to higher layers often outweigh the effect of error propagation on SER. This is consistent with our observation that also the full-fledged ordering algorithm in DiffSIC often places high priority users at higher layers.

The pseudo-code for our heuristic solution is shown in Table II. The scaling of SNRs is done by multiplying the noise enhancement factor $\mathbf{\Gamma}_{ii}$ for user i with the relative priority $(c_i - \min_{u\in\mathcal{U}}\{c_u\})$ (Table II, lines 7,14), where $\mathcal{U}$ is the set of users still to be ordered, and a sensitivity parameter $S \in [0, 1]$. The sensitivity parameter balances the influence of SNR ($1/\mathbf{\Gamma}_{ii}$) and user priority c_i on the detection order. More specifically, the scaling is designed such that when $S = 0$, no differentiation is attained, and the algorithm behaves exactly as V-BLAST in determining the order of detection for the first F users, whereas when $S \to 1$, the resulting order of detection is mostly determined by the users' priorities with V-BLAST being utilized only if equal priorities are present. If $S = 1$, sorting is done purely according to priorities. As an example, consider a 4×4 system where users' priorities are $\boldsymbol{c} = [0, 0.25, 0.50, 1.0]$ and $S = 0.5$. The total scaling vector at the first level (Table II, Line 8, for $F = 0$) will be $(1 - S) + S(\boldsymbol{c} - \min\{\boldsymbol{c}\}) = [0.50, 0.63, 0.75, 1.0]$. Thus, the noise enhancement term is amplified for users with higher priorities, which discourages the early detection of these users.

Since $N_{\max}$ is not necessarily a factorial number, the pseudo-code in Table II contains two stages, where F users are ordered first and then D selections for the $(F + 1)$st user are allowed such that $(M_{\mathrm{t}} - (F + 1))!D \leq N_{\max}$ (Table II, lines 12-15). Numerical results in Section VI will illustrate the complexity-performance tradeoff achievable with this approximation for DiffSIC.

TABLE II: Determine a reduced set of detection orders for DiffSIC

Input: Sensitivity parameter S, users' priorities $\boldsymbol{c} = [c_1, \ldots, c_{M_{\mathrm{t}}}]$
Output: $[k_1, \ldots, k_F, k^l_{F+1}]$, $l \in [1, 2, \ldots, D]$

1: // $\boldsymbol{H}^+$ denotes the pseudo inverse of $\boldsymbol{H}$,
2: // $\boldsymbol{H}_{\bar{k}_i}$ is the "deflated" version of $\boldsymbol{H}$, in which columns $k_1, k_2 \cdots k_i$ have been zeroed
3: Initialize $k_0 = 0$, $\mathcal{U} = \{1, \ldots, M_{\mathrm{t}}\}$, $F = 0$
4: // First stage
5: **while** $((M_{\mathrm{t}} - (F + 1))! > N_{\max})$ **do**
6: $\quad \mathbf{\Gamma} = \boldsymbol{H}^+_{\bar{k}_F}(\boldsymbol{H}^+_{\bar{k}_F})^H$
7: $\quad k_{F+1} = \underset{i\in\mathcal{U}}{\operatorname{argmin}} \left\{ \mathbf{\Gamma}_{ii} \left[(1 - S) + S \left(c_i - \min_{u\in\mathcal{U}}\{c_u\} \right) \right] \right\}$
8: $\quad \mathcal{U} := \mathcal{U} \setminus k_{F+1}$
9: $\quad F := F + 1$
10: **end while**
11: // second stage
12: $D = \lfloor N_{\max}/(M_T - (F + 1))! \rfloor$
13: **for** $l = 1$ to D **do**
14: $\quad k^l_{F+1} = \underset{i\in\mathcal{U}\setminus\{k^1_{F+1},\ldots,k^{l-1}_{F+1}\}}{\operatorname{argmin}} \left\{ \mathbf{\Gamma}_{ii} \left[(1-S)+S \left(c_i - \min_{u\in\mathcal{U}}\{c_u\} \right) \right] \right\}$
15: **end for**
16: // The detection orders considered by DiffSIC start with $[k_1, \ldots, k_F, k^l_{F+1}]$, $l \in [1, 2, \ldots, D]$

V. Performance Under Channel Estimation Errors

In the formulation of DiffSIC we have assumed perfect up-link channel estimation at the receiver. However, channel estimation errors can lead to serious performance degradation as they not only affect data estimation but also the decision on the order of detection to be used. While this is true for general SIC receivers, such as V-BLAST, one could expect stronger degradations for DiffSIC, which relies on accurate SER estimation taking error propagation into account. It is therefore relevant to consider the effect of channel estimation errors on the performance of DiffSIC.

Towards this end, we assume that the users transmit pilot sequences of length P, which we organize as the rows of the $M_{\mathrm{t}} \times P$ matrix $\boldsymbol{S}_p$, and the corresponding received signal is

$$\boldsymbol{R}_p = \boldsymbol{H}\boldsymbol{S}_p + \boldsymbol{n} \,. \tag{19}$$

Based on $\boldsymbol{R}_p$ the receiver performs channel estimation, and the estimated channel matrix is used for subsequent data detection. Making the often used assumption that the elements of $\boldsymbol{H}$ are circularly symmetric complex Gaussian random variables, then it has been shown in [22] that maximum-likelihood (ML) and MMSE channel estimation with subsequent ML detection and joint ML processing of pilot and data signal can be cast into the same framework considering the equivalent channel model

$$\boldsymbol{r} = \tilde{\boldsymbol{H}}\boldsymbol{a} + \boldsymbol{\Delta H}\boldsymbol{a} + \boldsymbol{n} = \tilde{\boldsymbol{H}}\boldsymbol{a} + \boldsymbol{v} \,, \tag{20}$$

where $\tilde{\boldsymbol{H}}$ is the MMSE channel estimate, $\boldsymbol{\Delta H} = \boldsymbol{H} - \tilde{\boldsymbol{H}}$ is the estimation error, which is independent of $\tilde{\boldsymbol{H}}$, and $\boldsymbol{v} = \boldsymbol{\Delta H}\boldsymbol{a} + \boldsymbol{n}$. Furthermore, if the elements of $\boldsymbol{H}$ are i.i.d. with variance σ^2_H, the pilot sequences are orthogonal, and constant modulus data signaling, i.e., 4QAM, is used, then the elements of the effective noise vector $\boldsymbol{v}$ are also i.i.d. circularly symmetric complex Gaussian distributed with variance

$\sigma_v^2 = M_\mathrm{t} E_s \sigma_{\Delta H}^2 + \sigma_n^2$, where $\sigma_{\Delta H}^2 = 1/(E_s P \sigma_n^{-2} + \sigma_H^{-2})$ is the variance of the elements of $\boldsymbol{\Delta H}$. Hence, in this case, any SIC detector, including DiffSIC, can use the equivalent system model in (20) with the MMSE channel estimate $\tilde{\boldsymbol{H}}$, and the effect of pilot-symbol based channel estimation is fully accounted for by assuming the equivalent received SNR

$$\frac{\mathbb{E}\{\|\tilde{\boldsymbol{H}}\boldsymbol{a}\|_2^2\}}{\mathbb{E}\{\|\boldsymbol{v}\|_2^2\}} = \gamma \cdot \frac{P/M_\mathrm{t}}{1 + P/M_\mathrm{t} + 1/\gamma}\,, \tag{21}$$

where $\gamma = \frac{M_\mathrm{t} E_s \sigma_H^2}{\sigma_n^2}$ is the received SNR with perfect channel knowledge and the factor $\frac{P/M_\mathrm{t}}{1+P/M_\mathrm{t}+1/\gamma}$ is the penalty due to the estimation error. Since this factor approaches a constant for increasing SNR γ, we conclude that performance *differences* between DiffSIC and V-BLAST are essentially maintained regardless of the quality of channel estimation.

In the case of non-constant modulus transmission the variance of the effective noise becomes data dependent. A pragmatic approach is to still apply (20) with the assumption of i.i.d. elements of $\boldsymbol{v}$ with variance σ_v^2 given above. Simulation results presented in the next section indicate that also in this case the performance difference between DiffSIC and V-BLAST is maintained.

VI. Performance Results

In this section, we present a number of numerical results to demonstrate the benefits of DiffSIC. Unless otherwise specified, we assume a 4×4 multiple-user system, where $M_\mathrm{t} = 4$ different users share the up-link to a base station that is equipped with $M_\mathrm{r} = 4$ receive antennas and employs ZF-SIC. The channel coefficients are modeled as i.i.d. circularly symmetric complex Gaussian random variables. The SNR-axis in the following figures refers to the SNR per antenna, i.e., $\gamma/M_\mathrm{t} = E_s\sigma_H^2/\sigma_n^2$.

For the first set of results, we consider a single channel realization to illustrate the accuracy of the error-rate analysis and the potential of the DiffSIC algorithm. In particular, we apply the randomly generated channel realization ($\mathrm{j} = \sqrt{-1}$)

$$\boldsymbol{H} = \begin{bmatrix} 0.32{-}0.17\mathrm{j} & {-}0.31{+}0.05\mathrm{j} & 1.52{-}0.19\mathrm{j} & {-}0.77{+}1.42\mathrm{j} \\ 0.78{+}0.19\mathrm{j} & 0.89{+}0.13\mathrm{j} & 0.14{-}0.67\mathrm{j} & {-}0.11{+}1.09\mathrm{j} \\ 0.94{+}0.42\mathrm{j} & 0.76{+}0.26\mathrm{j} & 0.23{+}0.68\mathrm{j} & 0.27{-}0.22\mathrm{j} \\ {-}0.63{-}0.80\mathrm{j} & {-}0.49{-}0.41\mathrm{j} & 0.10{-}0.88\mathrm{j} & {-}0.72{-}0.04\mathrm{j} \end{bmatrix}.$$

Figures 2 and 3 compare the individual SER results for the four users obtained with the analysis from Section III-A to those obtained through Monte Carlo simulation assuming a fixed sequential order of detection. In Figure 2, we observe that the simulation results perfectly match the calculated SER values for all users when transmission with 4-QAM is assumed. In the case of the 16-QAM constellation in Figure 3, we note some discrepancies between analytical and simulation results, which are due to only considering errors between nearest-neighbor signal points in the error propagation model as devised in (6). However, it can be seen that this only affects the SER analysis at high SER values and the discrepancies quickly diminish for low SERs usually of interest. For the sake of clarity, we show results for 4-QAM transmission in the following, but we note that the conclusions made are valid for general QAM constellations.

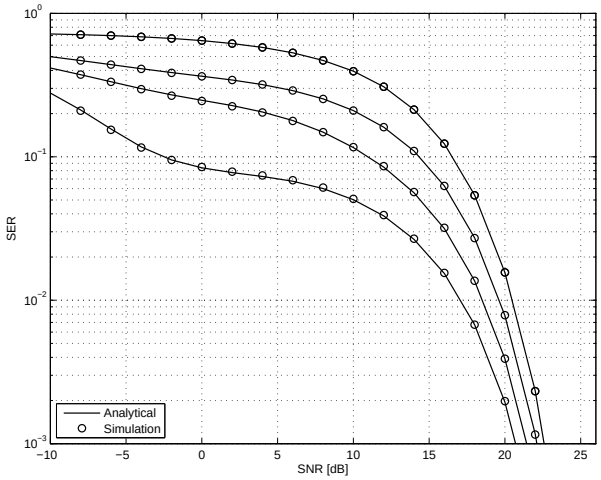

Fig. 2: Comparison of analytical and simulated SER performance results for one fixed channel realization. 4-QAM signal constellation and ZF-SIC detector using fixed order of detection.

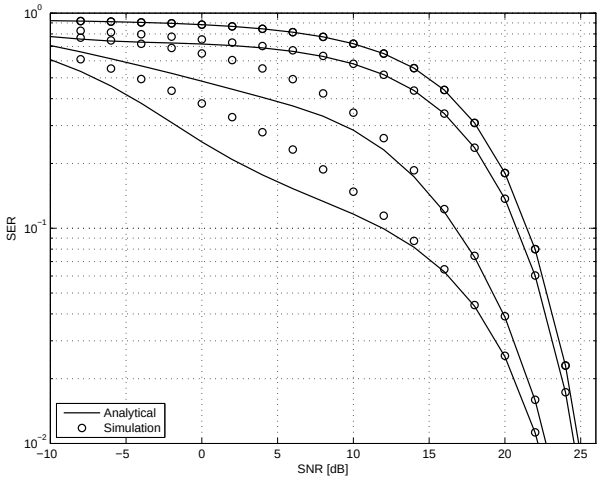

Fig. 3: Comparison of analytical and simulated SER performance results for one fixed channel realization. 16-QAM signal constellation and ZF-SIC detector using fixed order of detection.

The SER calculation can be made much faster by adopting the low-complexity SER approximation introduced in Section IV-A. Figure 4 compares the performance of our SER approximation method from Table I (Method 1) to a reduced complexity SER calculation technique following the suggestions in [13] (Method 2) in which error sequences with early errors are considered first. The figure shows the relative deviation of the approximated SER from the actual SER for user 4 (detected last in the detection chain) for different SNR values. It can be observed that our algorithm achieves a tight SER approximation much faster than Method 2 while, at the same time, the number of error sequences that are explored is significantly reduced. For example, only 10% of the total number of error sequences is sufficient to bring down the deviation from the actual SER to about 5% at an SNR of 10 dB.

Having confirmed the accuracy of the semi-analytical SER expressions and the efficiency of the proposed approximation, we now shift our attention to the potential of the DiffSIC algorithm. To this end, Figure 5 shows the SER-curves for

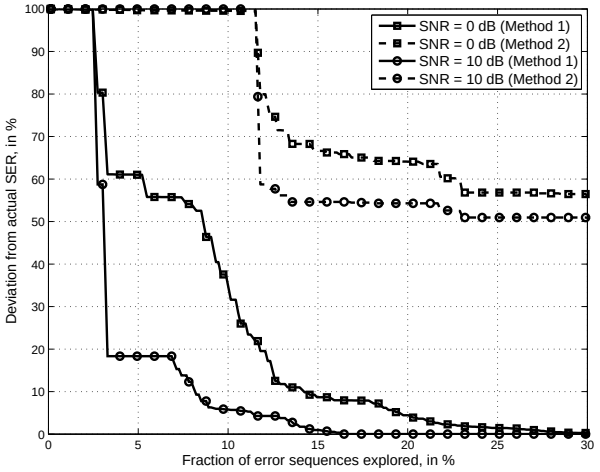

Fig. 4: Comparison of the efficacy of reduced complexity SER approximations. SER approximation method from Table I (Method 1) and SER approximation by considering error sequences with errors at lower layers first (Method 2). SER for user 4 is shown. The total number of error sequences is $3^6 = 729$. 4-QAM signal constellation and ZF-SIC detector.

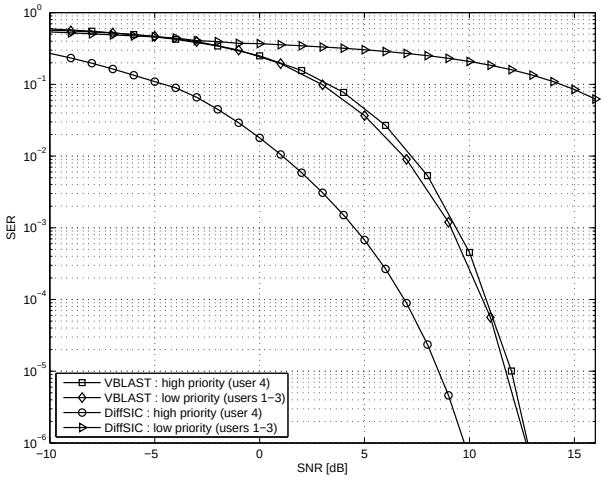

Fig. 5: SER performance comparison between DiffSIC and V-BLAST for one fixed channel realization. User priorities are $\boldsymbol{c} = [0, 0, 0, 1]$. 4-QAM signal constellation and ZF-SIC detector.

the same scenario as in Figure 2, but with ordering of users according to the channel realization (V-BLAST) and with DiffSIC taking user priorities into account. In this example, user 4 is the only high priority user with a priority indicator of $c_4 = 1$. The other three users are best effort with priority levels set to $c_i = 0$, $i = 1, 2, 3$. We observe that the high-priority user enjoys a significant SER advantage of several orders of magnitude under DiffSIC compared to V-BLAST. This advantage will reflect substantially on the user's service experience. Certainly, these gains come at the expense of low priority, best effort users, whose performance degradation depends on the particular channel realization. For the example shown in Figure 5 we observe that low priority users suffer a substantial degradation compared to V-BLAST as a result of their low class of service level. But the very purpose of DiffSIC is to enable the *receiver* to prefer some users over others, according to priority assignments, and the accomplishment of this task is evidenced in Figure 5.

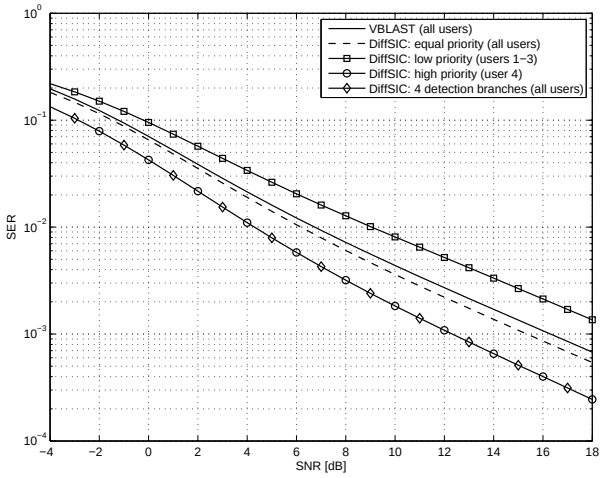

Fig. 6: Average SER performance comparison between DiffSIC and V-BLAST. User priorities are $\boldsymbol{c} = [0, 0, 0, 1]$. 4-QAM signal constellation and ZF-SIC detector.

In the second set of results, we consider the average SER performance for fading channels. In Figure 6 we compare the average SER for DiffSIC and V-BLAST. A number of interesting conclusions can be drawn from this figure. First, for the case of equal priority users, it can be seen that DiffSIC slightly outperforms the V-BLAST algorithm. This confirms that the V-BLAST ordering is sub-optimal yet surprisingly powerful given the low computational complexity it enjoys. Second, for the case of users with unequal priorities, the preferable treatment of the high priority user under DiffSIC provides it with a clear advantage compared to V-BLAST, e.g., an SNR advantage of 4 dB at SER of 10^{-3}. Third, if four parallel detection branches are used, each of which applies the DiffSIC optimal order for one of the users, then this 4 dB gain over V-BLAST is achieved for *all* users. The corresponding SER curve in Figure 6 exactly coincides with the SER curve for the high priority user in a single-branch DiffSIC detector.

The SNR gains of DiffSIC over V-BLAST are also present when MMSE-SIC detectors are used at the receiver. In Figure 7 we consider a 4×4 system, where user 4 is the only high priority user and MMSE-SIC is used at the receiver. In this example, the high priority user enjoys an about 4 dB SNR gain at SER $= 10^{-4}$ when DiffSIC is employed instead of V-BLAST. As shown before, the full SNR gains accomplished for the high-priority user could be extended to all users if multiple detection chains were available at the receiver.

We now consider the incorporation of the algorithms in Tables I and II from Section IV to reduce the computational complexity of DiffSIC. As before, the priority profile $\boldsymbol{c} = [0, 0, 0, 1]$ is chosen. Figure 8 shows the effect of using the SER approximation from Table I in determining the order of detection on the SER performance of the high priority user compared to V-BLAST. It is clear that the more error sequences are explored by the algorithm the wider the differentiation gap gets. However, we observe from Figure 8 that the major part of the gains is realized with only a small fraction of the total number of error sequences being considered. More specifically, we are able to attain almost the full advantage of

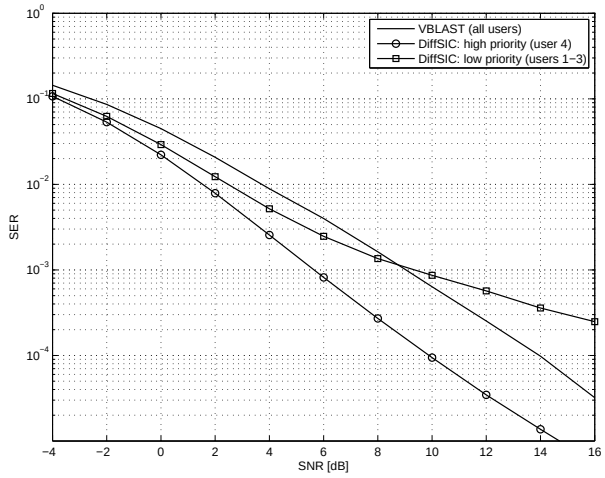

Fig. 7: Average SER performance comparison between DiffSIC and V-BLAST. $M_{\mathrm{t}} = M_{\mathrm{r}} = 4$. User priorities are $\boldsymbol{c} = [0, 0, 0, 1]$. 4-QAM signal constellation and MMSE-SIC detector.

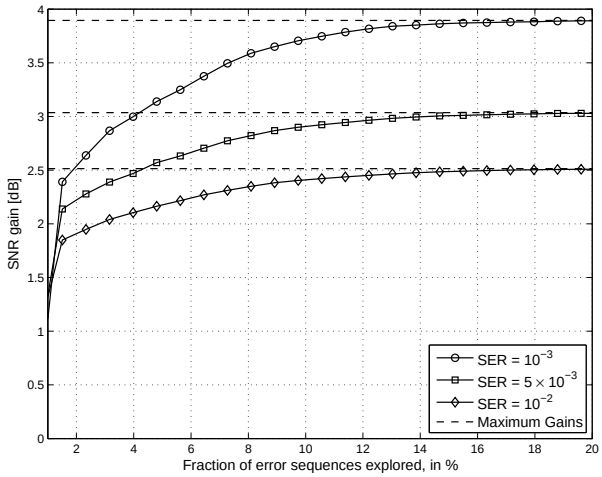

Fig. 8: Average SNR gain for high priority user with DiffSIC over V-BLAST when SER approximation according to Table I is used. User priorities are $\boldsymbol{c} = [0, 0, 0, 1]$. 4-QAM signal constellation and ZF-SIC detector.

DiffSIC at only 10% of the computational complexity, which is consistent with the SER results shown in Figure 4. Next, Figure 9 shows the SNR gains of the high-priority user for a target SER of 10^{-3} as a function of sensitivity parameter S and the maximal number of detection orders $N_{\max}$. Note that the total number of orders is $(M_{\mathrm{t}} = 4)! = 24$. We observe that already a good fraction of the maximal gain of about 3.9 dB (see Figure 8) is achieved with relatively few orders. Even a single order allows for notable gains of up to almost 2 dB. For the considered priority profile $\boldsymbol{c} = [0, 0, 0, 1]$, the sensitivity parameter $S \to 1$ yields the best performance on average. This corresponds to pushing the high priority user to the end of the detection chain and V-BLAST ordering for lower layers whose order is then fixed in DiffSIC.

The effect of the sensitivity parameter is more apparent when multiple priority levels are present. We therefore present in Figure 10 the same plot as in Figure 9 but with users having four different priority levels, namely $\boldsymbol{c} = [0, 0.25, 0.5, 1]$. It can be seen that a sensitivity parameter $0 < S < 1$ which balances the effects of the channel quality and user priority is preferable. While the optimal value of S changes with system configuration, i.e., user priorities $\boldsymbol{c}$ and maximal number of orders $N_{\max}$, these values can be pre-calculated off-line and assigned accordingly.

The two approximation techniques proposed in this paper can also be used in combination to further reduce the computational complexity of DiffSIC. The 3-dimensional plot in Figure 11 shows the average SNR gains the high priority user achieves under DiffSIC over V-BLAST when both reduced complexity approximations are utilized. The figure clearly shows that by adopting both algorithms simultaneously we can reduce the computational complexity substantially without loosing much on the SNR gains. We thus conclude the complexity-reduced DiffSIC is an attractive tool to accomplish user differentiation at the receiver in an up-link multiple-user system.

Finally, we provide simulation results that support the use of the equivalent system model in (20) with appropriate

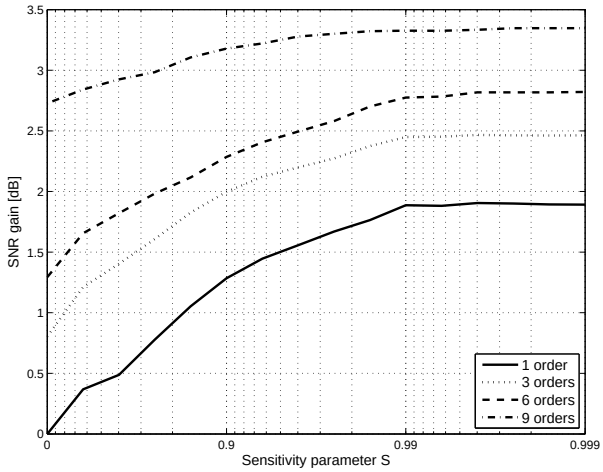

Fig. 9: Average SNR gain for high priority user with DiffSIC over V-BLAST when a reduced number of orders $N_{\max}$ is used according to Table II vs sensitivity parameter S. User priorities are $\boldsymbol{c} = [0, 0, 0, 1]$. 4-QAM signal constellation and ZF-SIC detector.

SNR shifts even for non-constant modulus transmission. In Figure 12 we consider the single channel realization $\boldsymbol{H}$ from the beginning of this section, and we show the SER performance curves for V-BLAST and DiffSIC for a 16-QAM transmission under the assumption of perfect and imperfect channel estimation. For the case in which channel estimation errors occur, we assume a transmit pilot sequence length of $P = 5$, and the channel $\tilde{\boldsymbol{H}}$ is a damped version of the channel $\boldsymbol{H}$ such that $\tilde{\boldsymbol{H}} = \sqrt{\frac{\sigma_H^2 - \sigma_{\Delta H}^2}{\sigma_H^2}}\boldsymbol{H}$ to maintain a variance of σ_H^2 for the sum $\tilde{\boldsymbol{H}} + \boldsymbol{\Delta H}$. The figure clearly shows how the shifted version of the SER curves (according to (21)) under channel estimation errors coincide with the corresponding SER curves under the perfect channel estimation assumption. Thus, the performance gap between V-BLAST and DiffSIC is maintained regardless of the channel estimation quality.

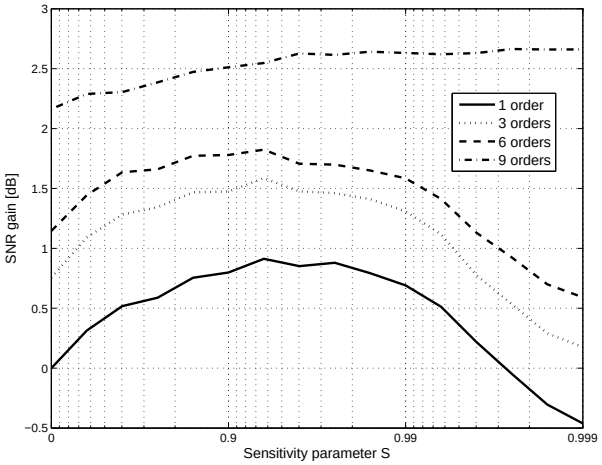

Fig. 10: Average SNR gain for high priority user with DiffSIC over V-BLAST when a reduced number of orders $N_{\max}$ is used according to Table II vs sensitivity parameter S. User priorities are $\boldsymbol{c} = [0, 0.25, 0.5, 1]$. 4-QAM signal constellation and ZF-SIC detector.

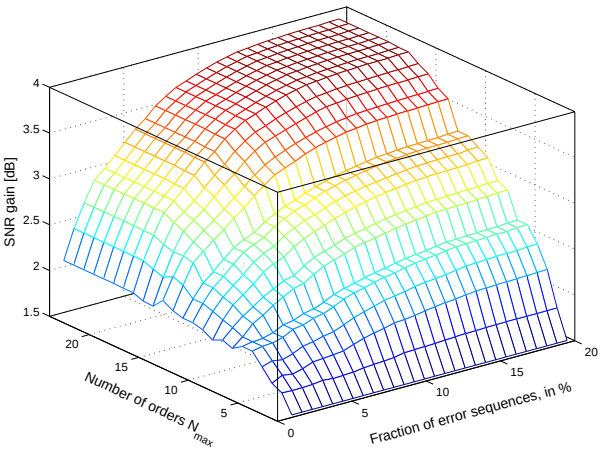

Fig. 11: Average SNR gain for high priority user with DiffSIC over V-BLAST when SER approximation according to Table I and a reduced number of orders $N_{\max}$ is used according to Table II ($S = 0.999$). 4-QAM signal constellation and ZF-SIC detector.

VII. Conclusion

In this paper, we have introduced the new Differentiated Successive Interference Cancellation (DiffSIC) ordering technique for up-link multiple-user systems. DiffSIC relies on the SER evaluation for ZF-SIC and MMSE-SIC, for which we have presented semi-analytical expressions, to find the order of detection that best fits the users' needs. We have also presented an SER approximation method, which is interesting in its own right and helps to achieve the differentiation gains with reduced computational complexity. In addition, we have devised a heuristic ordering algorithm to be used with DiffSIC, which takes channel quality and user priorities into account. We have shown numerical and simulation results which demonstrate that DiffSIC is capable of differentiating users according to their class of service. In particular, DiffSIC improves the SER performance of high-priority users significantly compared to those achieved with V-BLAST receivers. Furthermore, if DiffSIC is applied in combination with multiple detectors, these SER performance enhancements can be realized for multiple

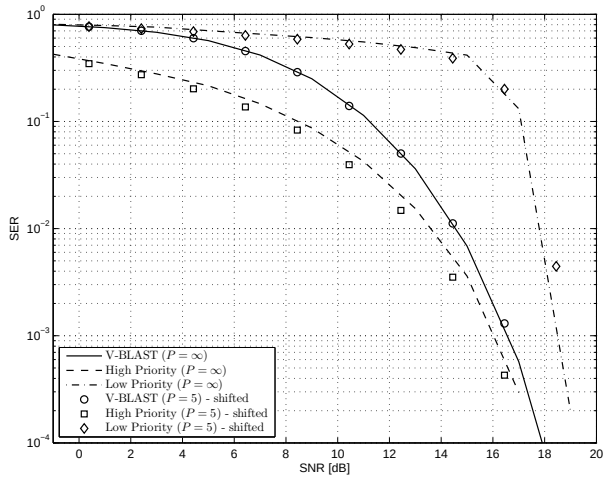

Fig. 12: SER performance of DiffSIC and V-BLAST for perfect ($P = \infty$) and imperfect ($P = 5$) channel estimation (SNR for imperfect channel estimation is shifted for proper comparison). One fixed channel realization with user priorities of $\boldsymbol{c} = [0, 0, 0, 1]$, 16-QAM signal constellation and ZF-SIC detector.

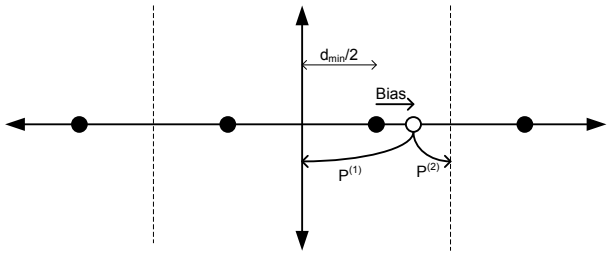

Fig. 13: Effect of signal bias on error probability of PAM signals.

users. We thus believe that DiffSIC is a powerful detection tool to accomplish service differentiation and performance improvement in general.

Appendix
Derivation of Error Probability Expressions for ZF-SIC PAM Signals

The effect of error propagation (see (6)) in ZF-SIC can be viewed as a signal bias that can affect the way error probabilities are calculated for PAM signals in Additive White Gaussian Noise (AWGN) channels. Because of this signal bias, the error probability to the left side of the signal constellation point is different from the error probability to the right side of it. These probabilities become identical if no error propagation was present. See Figure 13 for an illustration of these two different probabilities.

For each one of the $L - 2$ inner signal points, the error probability to the left and to the right of the signal point are

$$P^{(1)} = Q\left(\frac{d_{\min}/2 + \text{Bias}}{\sqrt{\sigma^2/2}}\right) \tag{22}$$

and

$$P^{(2)} = Q\left(\frac{d_{\min}/2 - \text{Bias}}{\sqrt{\sigma^2/2}}\right), \tag{23}$$

respectively. For the right most signal point, only $P^{(1)}$ is relevant, while for the left most signal point, only $P^{(2)}$ is

relevant. Thus the average SER can be written as

$$P = \frac{1}{L}\left\{(L-1)P^{(1)} + (L-1)P^{(2)}\right\} = \frac{L-1}{L}\left(P^{(1)} + P^{(2)}\right) \quad (24)$$

Substituting Bias $= \sum_{k=1}^{i-1} \bar{b}_{ik} e_k$ and $\sigma^2 = \sum_{j=1}^{M_r} \bar{f}_{ij}^2 \sigma_n^2$ for ZF-SIC, we get the equations in (8) and (9).

REFERENCES

[1] S. Verdu, *Multiuser Detection*. Cambridge University Press, 1998.

[2] H. Huang, S. Schwartz, and S. Verdu, "Combined multipath and spatial resolution for multiuser detection: Potentials and problems," in *Proc. IEEE Int. Symp. Inform. Theory*, 1995, p. 380.

[3] P. W. Wolniansky, G. J. Foschini, G. D. Golden, and R. A. Yalenzuela, "V-BLAST: An architecture for realizing very high data rates over the rich-scattering wireless channel," in *Proc. URSI Int. Symp. Signals, Systems, and Electronics*, 1998.

[4] V. Srivastava and M. Motani, "Cross-layer design: a survey and the road ahead," *IEEE Commun. Mag.*, vol. 43, pp. 112–119, 2005.

[5] P. Bhagwat, P. P. Bhattacharya, A. Krishna, and S. K. Tripathi, "Enhancing throughput over wireless LANs using channel state dependent packet scheduling," in *Proc. IEEE Conf. on Computer Commun. (INFOCOM)*, 1996, pp. 1133–1140.

[6] R. Zhang, Y.-C. Liang, R. Narasimhan, and J. Cioffi, "Approaching MIMO-OFDM capacity with per-antenna power and rate feedback," *IEEE J. Select. Areas Commun.*, vol. 25, no. 7, pp. 1284–1297, September 2007.

[7] R. Zhang and J. Cioffi, "Approaching MIMO-OFDM capacity with zero-forcing V-BLAST decoding and optimized power, rate, and antenna-mapping feedback," *IEEE Trans. Signal Processing*, vol. 56, no. 10, pp. 5191–5203, Oct. 2008.

[8] J. R. Barry, E. A. Lee, and D. G. Messerschmitt, *Digital Communication*, 3rd ed. Kluwer, 2004.

[9] M. Siti and M. Fitz, "A novel soft-output layered orthogonal lattice detector for multiple antenna communications," in *Proc. IEEE Int. Conf. on Commun.*, vol. 4, June 2006, pp. 1686–1691.

[10] L. Azzam and E. Ayanoglu, "Reduced complexity sphere decoding for square QAM via a new lattice representation," in *Proc. IEEE Global Telecommun. Conf.*, Nov. 2007, pp. 4242–4246.

[11] N. Prasad and M. K. Varanasi, "Analysis of decision feedback detection for MIMO rayleigh-fading channels and the optimization of power and rate allocations," *IEEE Trans. Inform. Theory*, vol. 50, pp. 1009–1025, Jun. 2004.

[12] S. Loyka and F. Gagnon, "Performance analysis of the V-BLAST algorithm: An analytical approach," *IEEE Trans. Wireless Commun.*, vol. 3, no. 4, pp. 1326–1337, Jul. 2004.

[13] ——, "V-BLAST without optimal ordering: analytical performance evaluation for Rayleigh fading channels," *IEEE Trans. Commun.*, vol. 54, no. 6, pp. 1109–1120, Jun. 2006.

[14] M. Chiani, D. Dardari, and M. Simon, "New exponential bounds and approximations for the computation of error probability in fading channels," *IEEE Trans. Wireless Commun.*, vol. 2, no. 4, pp. 840–845, Jul. 2003.

[15] S. Kim and K. Kim, "Log-likelihood-ratio-based detection ordering in V-BLAST," *IEEE Trans. Commun.*, vol. 54, pp. 302–307, Feb. 2006.

[16] G. Barriac and U. Madhow, "PASIC: A new paradigm for low-complexity multiuser detection," in *Proc. Conf. on Inform. Sci. and Syst.*, The Johns Hopkins University, Mar. 2001.

[17] R. de Lamare and R. Sampaio-Neto, "Minimum mean-squared error iterative successive parallel arbitrated decision feedback detectors for DS-CDMA systems," *IEEE Trans. Commun.*, vol. 56, no. 5, pp. 778–789, May 2008.

[18] R. H. Bacon, "Approximations to multivariate normal orthant probabilities," *The Annals of Mathematical Statistics*, vol. 34, no. 1, pp. 191–198, 1963.

[19] A. Solow, "A method for approximating multivariate normal orthant probabilities," *Journal of Statistical Computation and Simulation*, vol. 37, pp. 225–229, 1990.

[20] H. Joe, "Approximations to multivariate normal rectangle probabilities based on conditional expectations," *Journal of the American Statistical Association*, vol. 90, no. 431, pp. 957–964, 1995.

[21] V. Kostina and S. Loyka, "On optimum power allocation for the V-BLAST," *IEEE Trans. Commun.*, vol. 56, no. 6, pp. 999–1012, Jun. 2008.

[22] J. Giese and M. Skoglund, "Space-time constellation design for partial CSI at the receiver," *IEEE Trans. Inform. Theory*, vol. 53, no. 8, pp. 2715–2731, Aug. 2007.

Tariq Al-Khasib (S'99) received the B.S. degree in Electrical and Computer Engineering from Jordan University of Science and Technology, Irbid, Jordan, in 2001, and the M.A.Sc. degree in Electrical and Computer Engineering from the University of British Columbia, Vancouver, BC, Canada, in 2004. He is currently a Ph.D. candidate in the department of Electrical and Computer Engineering, University of British Columbia, Vancouver, Canada. His current research interests include MIMO techneques for wireless communications, Cognitive Radio systems, and robust optimization for multiple-user communication systems.

Lutz Lampe (M'02, SM'08) received the Diplom (Univ.) and the Ph.D. degrees in electrical engineering from the University of Erlangen, Germany, in 1998 and 2002, respectively. Since 2003 he has been with the Department of Electrical and Computer Engineering at the University of British Columbia, where he is currently an Associate Professor.

He is co-recipient of the Eurasip Signal Processing Journal Best Paper Award 2005 and the Best Paper Award at the 2006 IEEE International Conference on Ultra-Wideband (ICUWB). In 2003, he received the Dissertation Award of the German Society of Information Techniques (ITG). He was awarded the UBC Killam Research Prize in 2008, the Friedrich Wilhelm Bessel Research Award by the Alexander von Humboldt Foundation in 2009, and the UBC Charles A. McDowell Award of Excellence in Research in 2010.

He is an Editor for the IEEE Transactions on Wireless Communications and the International Journal on Electronics and Communications (AEUE), and he has served as Associate Editor for the IEEE Transactions on Vehicular Technology from 2004 to 2008. He is Vice-Chair of the IEEE Communications Society Technical Committee on Power Line Communications. He was General Chair of the 2005 International Symposium on Power Line Communications and the 2009 IEEE International Conference on Ultra-Wideband.

Hussein M. Alnuweiri (S'81, M'83) Currently a Professor in the Electrical and Computer Engineering Program at Texas A&M University at Qatar. His main research interests are related to mobile Internet technologies including Internet computing, multimedia communications, wireless protocols, routing and information dissemination algorithms for opportunistic networking, and quality of service provisioning and resource allocation in packet networks. He obtained his PhD in Electrical and Computer Engineering from the University of Southern California, and Master's Degree from the King Fahad University of Petroleum & Minerals. From 1991 to 2007 he was a professor in the Department of Electrical and Computer Engineering at the University of British Columbia. He served as a Canadian delegate to the ISO/IEC JTC1/SC29 Standards Committee (MPEG-4 Multimedia Delivery) from 2000 to 2006, where he worked within the MPEG-4 standardization is JTC1-SC29WG11 and the Ad-Hoc group involved in the development of the reference software is called IM1 AHG. He also represented the University of British Columbia at the ATM Forum, from 1996 to 1998. He is also an inventor with three issued U.S. patents on Arbitration Protocols and Weighted Fair Queuing algorithms.